

Hard X-Ray Flux Upper Limits of Central Compact Objects in Supernova Remnants

I. Erdeve¹, E. Kalemci², M. A. Alpar²

ABSTRACT

We searched for hard X-ray (20–300 keV) emission from nine central compact objects (CCOs) 1E 1207.4–5209, 1WGA J1713–3949, J082157.5–430017, J085201.4–461753, J1601–5133, J1613483–5055, J181852.0–150213, J185238.6+004020, and J232327.9+584843 with the *INTEGRAL* observatory. We applied spectral imaging analysis and did not detect any of the sources with luminosity upper limits in the range of 10^{33} – 10^{34} ergs/s in the 20–75 keV band. For nearby CCOs (< 4 kpc) the upper limit luminosities are an order of magnitude lower than the measured persistent hard X-ray luminosities of AXPs. This may indicate that the central compact objects are low magnetic field systems with fallback disks around them.

Subject headings: X-rays:stars – central compact objects – neutron stars – supernova remnants, stars individual: 1E 1207.4–5209, 1WGA J1713–3949, J082157.5–430017, J085201.4–461753, J1601–5133, J1613483–5055, J181852.0–150213, J185238.6+004020, J232327.9+584843

1. Introduction

X-ray observations have revealed groups of radio-quiet young (isolated) neutron stars: Anomalous X-ray Pulsars (AXPs), Soft Gamma Repeaters (SGRs), X-ray Dim Neutron Stars (XDNSs), and Central Compact Objects (CCOs). AXPs are known to emit pulsed X-rays below 10 keV with periods in the range ~ 5 –12s (see Kaspi & Gavriil 2004; Mereghetti 200, for a review). Their rate of rotational kinetic energy loss is well below the soft X-ray luminosity. They are believed to have exceptionally strong ($\gtrsim 10^{14}$ G) surface magnetic

¹Istanbul University, Science Institute, Department of Astronomy and Space Science, Beyazıt-Eminönü, 34452, İstanbul, Turkey

²Sabancı University, Orhanlı-Tuzla, İstanbul, 34956, Turkey.

field strengths, and are powered by magnetic field decay, hence they are called magnetars (Thompson et al. 2002; Güver et al. 2007).

Another model attributes the soft X-ray emission and spindown of persistent AXPs and SGRs and their newly discovered transient members to accretion torques from active fallback disks (Alpar 2001; Chatterjee et al. 2000; Ertan et al. 2007a; Ertan & Erkut 2007). During the supernova explosion, fallback of material from the progenitor may establish an accretion disk around the neutron star. Indeed a debris disk has been found around a young isolated neutron star, 4U 0142+61 (Wang et al. 2006, but also see Wang et al. 2007) whose properties explain the overall broadband data of the source (Ertan et al. 2007b).

Hard X-ray emission has been discovered from four AXPs between 20–300 keV (Molkov et al. 2004; Kuiper et al. 2004; den Hartog et al. 2004; Revnivtsev et al. 2004; Kuiper et al. 2006). The current models to explain this hard X-ray emission often invoke magnetar fields (Heyl & Hernquist 2005; Thompson & Beloborodov 2005; Baring & Harding 2007). Discovery of high energy emission from AXPs which are formerly known to have only soft emission prompted us to search for high energy emission from similar isolated neutron stars, especially the ones that may also have high magnetic fields.

One such group of young isolated neutron stars that have circumstantial evidence for having high magnetic fields are the CCOs. These are X-ray point sources which are found near the center of supernova remnants, show no radio counterpart, no pulsar wind nebula, and have thermal-like soft spectra. The soft X-ray spectra usually consist of thermal components with blackbody temperatures of 0.2–0.5 keV, X-ray luminosities $L_x \sim 10^{33} - 10^{34} \text{ erg s}^{-1}$ and characteristic sizes of 0.3–3 km (see Pavlov et al. 2004, for a review).

Some properties of these sources have been interpreted as a result of high magnetic fields in the past. For example, if the line features in 1E 1207.4–5209 are due to proton cyclotron absorption, the magnetic field of this source must be greater than 10^{14} G (Bignami et al. 2003). The same line features were also interpreted as fine structure splitting of He^+ under magnetar fields (Pavlov & Bezchastnov 2005). Krause et al. (2005) observed the SNR Cas A with the Spitzer Space Telescope and detected infrared echoes. One possible explanation for those features is magnetar type explosions and flares from the compact object J232327.9+584843 near the center of the SNR. Li (2007) studied 1E161348–5055 in SNR RCW 103 and suggested that it is either an isolated magnetar or a low-mass X-ray binary which survived the supernova event with a fallback disk.

On the other hand, there is also evidence for CCOs having normal/weak magnetic fields. Gotthelf & Halpern (2007) reported that measured spin-down rate of 1E 1207.4–5209 implies a magnetic field strength of $B_p < 3.3 \times 10^{11} \text{ G}$. The X-ray luminosity exceeds its rotational

energy loss rate. This indicates that luminosity arises from residual cooling and perhaps partly from accretion of supernova debris. Gotthelf & Halpern (2007) also suggested that the neutron star J232327.9+584843 may have undergone a one-time phase transition which powered the light echo.

Most of the properties of the CCOs can be understood if they are propellers (Alpar 2001). According to evolutionary scenarios with fallback disks, their periods are expected to be $P_{eq} < 1$ s corresponding to high-mass inflow rate. These periods that are smaller than those of AXPs suggest that they may be predecessors of AXPs (Alpar 2001). Although periods of most CCOs have not been observed yet, measured periods of two CCOs are consistent with this interpretation (period of the CCO 1E 1207.4–5209 is about 424 ms (Zavlin et al. 2000) and period of the CCO J185238.6+004020 is 105 ms (Gotthelf et al. 2005)). The period measurement, $P=7.5$ s for the source J160103.1–513353 (Park et al. 2006) has not been confirmed yet .

We present here the hard X-ray flux measurements of these nine CCOs and CCO candidates for an unbiased analysis (1E 1207.4–5209, 1WGA J1713–3949, J0002–6246, J082157.5–430017, J085201.4–461753, J1601–5133, J161348–5055, J181852.0–150213, J185238.6+004020, J232327.9+584843) with the ISGRI detector on *INTEGRAL*. We aim to understand the nature of their emission, and by comparing the hard X-ray properties to that of AXPs we want to investigate the connections between different types of isolated neutron stars.

2. Sources

One of the best investigated CCOs is 1E 1207.4–5209 in the SNR G296.5+10.0. It was discovered by Helfand & Becker (1984). It is located about $6'$ off the center of G296.5+10, at a distance of about 2 kpc. The soft X-ray energy spectrum is best modeled with a continuum blackbody component with temperature $kT \sim 0.14$ keV, and at least two broad absorption lines centered at 0.7 and 1.4 keV. Zavlin et al. (2000) observed 1E 1207.4–5209 with the Chandra X-ray Observatory and discovered a period of about 424 ms. The second Chandra observation provided an estimate of the period derivative, $\dot{P} \sim (0.7-3) \times 10^{-14} \text{ s s}^{-1}$ (Pavlov et al. 2002). The corresponding characteristic age of the pulsar, $P/2\dot{P} \sim 200-900$ kyr, is much larger than the estimated age of the SNR, ~ 7 kyr. It has been proposed that this discrepancy is due to glitches. Alternatively $P/2\dot{P}$ may be irrelevant as an age estimate because the \dot{P} is due to a fallback disk or a low mass binary companion. Using the *XMM-Newton* data Woods et al. (2006) claimed that the observed spin irregularities originated from the presence of a binary companion to 1E 1207.4–5209.

RX J1713–3946 is a shell-type SNR, embedded in the galactic plane. The remnant was discovered in X-rays with ROSAT, which also identified two point sources within the boundaries of the SNR shell (Pfeffermann & Aschenbach 1996). 1WGA J1713.4–3949, is located at the geometrical center of the SNR and no optical counterpart has been found within $10''$ of the ROSAT position (Slane et al. 1999). Chandra, XMM-Newton and RXTE observations showed that the X-ray spectrum of the source is well fitted by the sum of a blackbody component with a temperature of ~ 0.4 keV plus a power-law component with a photon index of ~ 4 (Lazendic et al. 2003).

The source J082157.5–430017, located about $6'$ off the center of SNR the Puppis A, was discovered with Einstein by Petre et al. (1982). Hui & Becker (2006) presented spectral analysis results using XMM-Newton and Chandra data. The observed point source is best described with a double blackbody model with temperatures $T_1 = (2.35 - 2.91) \times 10^6$ K, $T_2 = (4.84 - 5.3) \times 10^6$ K.

Pavlov et al. (2001) found a relatively bright source (J085201.4–461753) in the SNR Vela Junior (G266.1–1.2) with a flux of $\sim 2 \times 10^{-12}$ ergs $s^{-1} cm^{-2}$ in the 0.5–10 keV energy band using Chandra data. The spectrum of the source is best fitted with a blackbody model with temperature $kT = 404 \pm 5$ eV and radius of the emitting region $R = 0.28 \pm 0.01$ km at a distance of 1 kpc. Becker et al. (2006) did not find any pulsations to a 3σ upper limit for any pulsed fraction with XMM-Newton.

Park et al. (2006) discovered a point like source J160103.1–513353 at the center of Galactic SNR G330.2+1.0 with Chandra X-ray Observatory. The X-ray spectrum is fitted with a blackbody model with $kT \sim 0.49$ keV, implying a small emission region $R \sim 0.4$ km at distance of 5 kpc and estimated X-ray luminosity is $L_x \sim 1 \times 10^{33}$ ergs s^{-1} in the 1–10 keV energy band. They found a possible X-ray period of the source $P \approx 7.5$ s.

The first discovered radio-quiet X-ray point source, J161348–5055, was found in the young SNR RCW 103 by Tuohy & Garmire (1980). A period of 6 hr was found with both Chandra and ASCA (Garmire et al. 2000) and the X-ray observation have shown that its flux varies through a wide range. Sanwal et al. (2002) have found a 6.4 hr period and multiple dips in the X-ray light curve using Chandra ACIS data. Becker & Aschenbach (2002) reported the evidence of an eclipse from a light curve observed by *XMM-Newton*. All of these results suggest that J161348–5055 is an accreting object in a binary system. On the other hand De Luca et al. (2006) suggest that J161348–5055 may be a magnetar rotating at 6.67 hr with $B > 10^{15}$ G. Even with such magnetic field, a neutron star can not spin down to 6.7 hr via magnetic dipole radiation during the lifetime of the SNR. A supernova fallback disk is proposed to interact with the magnetar, providing additional propeller spin down torques (Li 2007).

Reynolds et al. (2006) discovered an X-ray point source J181852.0–150213 within SNR G15.9+0.2 with *Chandra*. The X-ray spectrum of the source is consistent with either a steep $\Gamma \sim 4$ power law or a $kT \sim 0.4$ keV blackbody and the neutral hydrogen column density is $N_H \sim 4 \times 10^{22} \text{ cm}^{-2}$.

A point-like source J185238.6+004020 found at the center of SNR Kes 79 (G33.6+0.1) by Seward et al. (2003) with *Chandra* ACIS. Gotthelf et al. (2005) discovered 105 ms X-ray pulsations from the source using *XMM-Newton* data, and using two observations of the pulsar, 6 days apart, they calculated $\dot{P} < 7 \times 10^{-14} \text{ s s}^{-1}$. The X-ray spectrum of the source is well fitted with a blackbody model with temperature $kT = 0.44 \pm 0.03$ keV, radius $R \approx 0.9$ km, and $L_{bol} = 3.7 \times 10^{33} \text{ ergs s}^{-1}$ assuming $d = 7.1$ kpc (Gotthelf et al. 2005).

The prototype of CCO, J232327.9+584843 was discovered near the center of SNR Casiopeia A in the first-light *Chandra* observation by Tananbaum (1999), and found later in the archival ROSAT and Einstein images. A blackbody fit to the observed *Chandra* ACIS spectrum shows a high temperature $kT \approx 0.5$ keV and a small effective radius $R \approx 0.4$ km, at the remnant’s estimated distance of 3.4 kpc (Reed et al. 1995), leading to suggestions of a neutron star with hot spots (Pavlov et al. 2000).

3. Instruments and Observations

The *INTEGRAL* Soft Gamma-Ray Imager (ISGRI) is the low-energy camera of the IBIS telescope (Lebrun 2003) on *INTEGRAL* and is sensitive between 20 keV and 1 MeV. It’s detector area is 2621 cm^2 made up of 16,384 CdTe pixels. The fully coded field of view is 9° , and the angular resolution is $\sim 13'$ (Gros et al. 2003). Table 1 shows the observations that are used in this study for imaging and spectral analysis. “Begin Date” and “End Date” show observation date of the first and the last revolution respectively. The properties of CCOs are shown in Table 2.

4. Analysis Methods

The *INTEGRAL* IBIS ISGRI imaging analysis (OSA 5.1) was applied in our study. We produced images in two energy bands (20–75 keV and 75–300 keV) for each source while restricting our science windows within 10° of the source. We eliminated images with poor quality and combined all clean science windows producing single sky mosaics for each source in these two energy bands. Comparing significance maps with flux maps in these sky mosaics, we obtained $3\text{-}\sigma$ flux upper limits for each source. For calculating upper limit

fluxes, we assumed a photon index of 1, based on the ISGRI hard X-ray spectra of AXPs.

5. Results

Except Cas A in the 20–75 keV range, none of the CCOs have been significantly detected with ISGRI despite large exposure times. For Cas A, we detected the young SNR. This SNR has already been detected between 40 – 120 keV energy range with CGRO/OSSE (The et al. 1996), with HEXTE on *RXTE* (Rothschild & Lingenfelter 2003), and with ISGRI (Renaud et al. 2006). With ISGRI’s imaging capabilities we cannot resolve the compact object from the SNR and therefore cannot provide reliable flux limits for this source in the 25-75 keV band. For all the other sources, the contribution of the SNR to hard X-rays is negligible. SNRs G296.5+10.0, G347.3-0.5, Puppis A (G260.4-3.4) and Vela Junior (G266.1-1.2) are not only large compared to the pixel size of ISGRI, but they are also soft. Similarly Kes 79 (G33.6+0.1) (Sun et al. 2002) and RCW 103 (G332.4-0.4) (Gotthelf et al. 1999) have too soft thermal spectra to contribute any significant emission to hard X-rays compared to our upper limits. As an example, G330.2+1.0 according to the srcut model parameters reported in Torii et al. (2006), can at most contribute 1% of the upper limit flux we derived for the source.

To compare the soft X-ray to hard X-ray emission, we took model parameters of the eight sources from the literature (Table 3) and simulated the soft spectra using XSPEC11. Then we combine these with flux upper limits. The overall spectra are shown in Figs 1 – 8.

We also compared CCO upper limit fluxes with the measured AXP high energy fluxes. To achieve a valid comparison, we normalized all AXP distances to those of CCOs and recalculated all flux values in the 20–75 keV and 75–300 keV energy band (we assumed a Crab spectrum of power law photon index $\Gamma=2.15$ and normalization $N=10.4$). We also calculated the hard X-ray luminosities of AXPs to compare with the CCOs in Table 4.

6. Discussion

There are a few models to explain hard X-ray emission from anomalous X-ray pulsars and soft gamma-ray repeaters, all invoking magnetar fields. One such mechanism is the fast-mode breakdown under very strong magnetic fields (Heyl & Hernquist 2005). An alternative model is proposed by Thompson & Beloborodov (2005), again invoking an energy release by ultra strong magnetic fields. In this case, there may be a heating of the surface layer through Langmuir turbulence producing high energy bremsstrahlung radiation. Another possibility

for the source of high energy emission is the acceleration of positrons under strong electric fields ~ 100 km from the star, and subsequent pair production and synchrotron emission. These models, while invoking high magnetic fields, also assume gaps that would create electric fields accelerating charged particles, and producing gamma-ray emission. Finally, according to Baring & Harding (2007), for a range of magnetic colatitudes proximate to the neutron star surface, resonant Compton scattering in strong magnetic fields can be extremely efficient for powering the AXP in hard X-rays.

In this work we have shown that the nearby (distance < 4 kpc) CCOs have hard X-ray luminosities which are at least an order of magnitude lower than the hard X-ray luminosities of AXPs. If hard X-ray emission from the isolated neutron stars occur only under strong magnetic fields as the current models claim, our work may indicate low magnetic fields for CCOs. Note that AXPs have comparable luminosities in soft and hard X-rays. If the hard X-ray emission is powered by a mechanism that also powers soft X-ray emission, we should have detected hard X-rays from nearby CCOs.

According to Alpar (2001) the similarity of rotation periods of the AXPs, SGRs and the XDNSs suggest a common mechanism with an asymptotic spin-down phase. This model proposes that AXPs, SGRs, XDNSs and CCOs constitute alternative subclasses of young neutron stars. The differences between them are due to mass inflow rates and possibly also due to differences in the dipole component of the magnetic field, independently of whether the total field at the surface is at magnetar values. The pulse periods may not be observable if the optical thickness to electron scattering of the material surrounding the star destroys the X-ray beaming (but also see Göğüş et al. 2007 in context of LMXBs), or if in the strong mass inflow regime destroys the modulation of the accretion and the accretion luminosity over the star's surface. This scenario may also explain the lack of hard X-ray emission from the CCOs, as strong mass accretion rate would short out any gaps that could provide acceleration of particles in the magnetosphere.

This work was supported by the research funds of the Istanbul University, project number T-84/15122006. This work was also supported by the European Commission 6th Framework Projects INDAM (International Reintegration Grant, MIRG-CT-2005-017203) and AS-TRONS (Transfer of Knowledge Project, MTKD-2006-42722). EK is partially supported by TÜBİTAK. EK is also supported by the Turkish Academy of Sciences (TÜBA) with a Young and Successful Scientist Award. Authors thank Steve Reynolds and Hakan Erkut for valuable discussions.

REFERENCES

- Alpar, A., 2001, ApJ, 554:1245-1254
- Baring, M. G., Harding, A. K., 2007, Ap&SS, 308:109-118
- Becker, W., Aschenbach, B., 2002, Proceedings of the 270. WE-Heraeus Seminar on: "Neutron Stars, Pulsars and Supernova Remnants", eds. W. Becker, H. Lesch, J. Trümper, MPE Report 278, pp. 64-86
- Becker, W., Hui, C. Y., Aschenbach, B., Iyudin, A., 2006, A&A
- Bignami, G. F., Caraveo, P. A., de Luca, A., Mereghetti, S., 2003, Nature, Volume 423, Issue 6941, pp. 725-727
- Cassam-Chenai, G., Decourchelle, A., Ballet, J., Sauvageot, J. L., Dubner, G., Giacani, E., 2004, A&A, 427, 199-216
- Chatterjee, P., Hernquist, L., Narayan, R., 2000, ApJ, 534:373-379
- De Luca, A., Caraveo, P. A., Mereghetti, S., Tiengo, A., Bignami, G. F., 2006, Sci, 313, 814
- Ertan, Ü., Alpar, M. A., Erkut, M. H., Ekşi, K. Y., Çalışkan, S., 2007, Ap&SS, 308:73-77
- Ertan, Ü., Erkut, M. H., Ekşi, K. Y., Alpar, M. A., 2007, ApJ, 657, 441E
- Ertan, Ü., Erkut, 2008, ApJ, 673, 1062-1066
- Garmire, G. P., Pavlov, G. G., Garmire, A. B., 2000, IAU Circ. 7350
- Göğüş, E., Alpar, A., Gilfanov, M., 2007, ApJ, 659, 580
- Gotthelf, E. V., Petre, R., Vasisht, G., 1999, ApJ, 514:L107-L110
- Gotthelf, E. V., Halpern, J. P., Seward, F. D., 2005, ApJ, 627:390-396
- Gotthelf, E. V., Halpern, J. P., 2007, arXiv:0711.1554v1
- Gros, A., Goldwurm, A., Cadolle-Bel, M., Goldoni, P., Rodriguez, J., Foschini, L., Del Santo, M., Blay, P., 2003, A&A, 411, L179
- Guseinov, O. H., Ankay, A., Tagieva, S. O., 2003, Serb. Astron., 167:93-110
- Guseinov, O. H., Ankay, A., Tagieva, S. O., 2004, Serb. Astron., 168:55-69
- Guseinov, O. H., Ankay, A., Tagieva, S. O., 2004, Serb. Astron., 169:65-82

- Güver, T., Özel, F., Göğüs, E., 2008, *ApJ*, 675, 1499-1504
- den Hartog, P. R., Kuiper, L., Hermsen, W., Vink, J., 2004, *ATEL* 293
- Halpern, J. P., Gotthelf, E. V., Camilo, F., Seward, F. D., 2007, 665, 1304-1310
- Helfand, D. J., Becker, R. H., 1984, *Nature*, 307, 215
- Heyl, J. S., Hernquist, L., 2005, *ApJ*, 618, 463
- Hui, C. Y., Becker, W., 2006, *A&A*, 454, 543-552
- Jahoda, K., Swank, J. H., Giles, A. B., Stark, M. J., Strohmayer, T., Zhang, W., 1996, *Proc SPIE* 2808, 59
- Kargaltsev, O., Pavlov, G. G., Sanwal, D., Garmire, G. P., 2002, *ApJ*, 580:L1060-L1064
- Kaspi, V. M., Gavriil, F. P., 2004, *Nuclear Physics B Proceedings Supplements*, 132, 456-465
- Krause, O., Rieke, G. H., Birkmann, S. M., Le Floch, E., Gordon, G. D., Egami, E., Biegging, J., Hughes, J. P., Young, E. T., Hinz, J. L., Quanz, S. P., Hines, D. C., 2005, *Science*, 1604
- Kuiper, L., Hermsen, W., Mendez, M., 2004, *ApJ*, 613:1173-1178
- Kuiper, L., Hermsen, W., den Hartog, P. R., Collmar, W. 2006, *ApJ*, 613:1173-1178
- Lazendic, J. S., Slane, P. O., Gaensler, B. M., Plucinsky, P. P., Hughes, J. P., Galloway, D. K., Crawford, F., 2003, *ApJ*, 593:L27-L30
- Lebrun, F., 2003, *A&A*, 411, L141
- Li, X. D., 2007, *ApJ*, 666, L81-L84
- Luca, A. D., Mereghetti, S., Caraveo, P. A., Moroni, M., Mignani, R. P., Bignami, G. F., 2004, *A&A*, 418, 625-637
- Mereghetti, S., in *The Neutron Star – Black Hole Connection*, ed. V. Connaughton, C. Kouveliotou, J. van Paradijs, & J. Ventura, NATO Advanced Study Institute, (arXiv:astro-ph/9911252v2)
- Molkov, S. V., Cherepashchuk, A. M., Lutovinov, A. A., Revnivtsev, M. G., Postnov, K. A., Sunyaev, R. A., 2004, *Astronomy Letters*, 30, 534

- Park, S., Mori, K., Kargaltsev, O., Slane, P. O., Hughes, J. P., Burrows, D. N., Garmire, G. P., Pavlov, G. G., 2006, *ApJ*, 653:L37-L40
- Pavlov, G. G., Zavlin, V. E., Aschenbach, J., Trümper, J., Sanwal, D., 2001, *ApJ*, 531:L53-L56
- Pavlov, G. G., Sanwal, D., Kızıltan, B., Garmire, G. P., 2001, *ApJ*, 559:L131-L134
- Pavlov, G. G., Zavlin, V. E., Sanwal, D., Trümper, J., 2002, *ApJ*, 569:L95-L98
- Pavlov, G. G., Sanwal, D., Teter, M. A., 2004, *IAU Symposium*, Vol.218
- Pavlov, G. G., Bezchastnov, V. G., 2005, *ApJ*, 635:L61-64
- Petre, R., Canizares, C. R., Kriss, G. A., Winkler, P. F., 1982, *ApJ*, 258:22-30
- Pfeffermann, E., Aschenbach, B., 1996, in *Roentgenstrahlungn from the Universe*.
- Reed, J. E., Herter, J. J., Fabian, A. C., Winkler, P. F., 1995, *ApJ*, 440, 706
- Renaud, M., Vink, J., Decourchelle, A., Lebrun, F., den Hartog, P. R., Terrier, R., Couvreur, C., Knödseder, J., Martin, P., Prantzos, N., Bykov, A. M., Bloemen, H., 2006, *ApJ*, 647:L41-L44
- Reynolds, S. P., Borkowski, K. J., Hwang, U., Harrus, I., Petre, R., Dubner, G., 2006, *ApJ*, 652:L45-L48
- Revnivtsev, C., Sunyaev, R., Varshalovich, D., Zheleznyakov, V., Cherepashchuk, A., Lutovinov, A., Churazov, E., Grebenev, S., Gilfanov, M., 2004, *Astronomy Letters*, 30, 382
- Rothschild, R. E., Lingenfelter, R. E., 2003, *ApJ*, 582:257-261
- Sanwal, D., Garmire, G. P., Garmire, A., Pavlov, G. G., Mignani, R., 2002, *BAAS*, 34,764
- Seward, F. D., Slane, P. O., Smith, R. K., Sun, M., 2003, *ApJ*, 584:414-417
- Slane, P., Gaensler, B. M., Dame, T. M., Hughes, J. P., Plucinsky, P. P., Green, A., 1999, *ApJ*, 525:357-367
- Sun, M., Seward, F., Smith, R., Slane, P., 2002, *APS*, APRN17036S
- Tananbaum, H., 1999, *IAU Circ.*, 7246

- The, L. S., Leising, M. D., Kurfess, J. D., Jojnson, W. N., Hartmann, D. H., Gehrels, N.,
Grove, J. E., Purcell, W. R., 1996 A&A Supplement Series, 120, 357-360
- Thompson, C., Duncan, R. C., 1996, Apj, 473:322-342
- Thompson, C., Lyutikov, M., Kulkarni, S. R., 2002, Apj, 574:332-355
- Thompson, C., Beloborodov, A. M., 2005, Apj, 634:565-569
- Torii, K., Uchida, H., Hasuike, K., Tsunemi, H., Yamaguchi, Y., Shibata, S., 2006, PASJ,
58L, 11T
- Tuohy, I., Garmire, G., 1980, Apj, 239,L107
- Ubertini, P., A&A, 411, L131
- Woods, P. M., Zavlin, V. E., Pavlov, G. G., 2006, arxiv
- Wang, Z., Chakrabarty, D., Kaplan, D., 2006, Nature, 440, 772
- Wang, Z., Kaplan, D., Chakrabarty, D., 2007, Apj, 655, 261
- Zavlin, V. E., Pavlov, G. G., Sanwal, D., Trümper, J., 2000, ApJ, 540:L25-L28

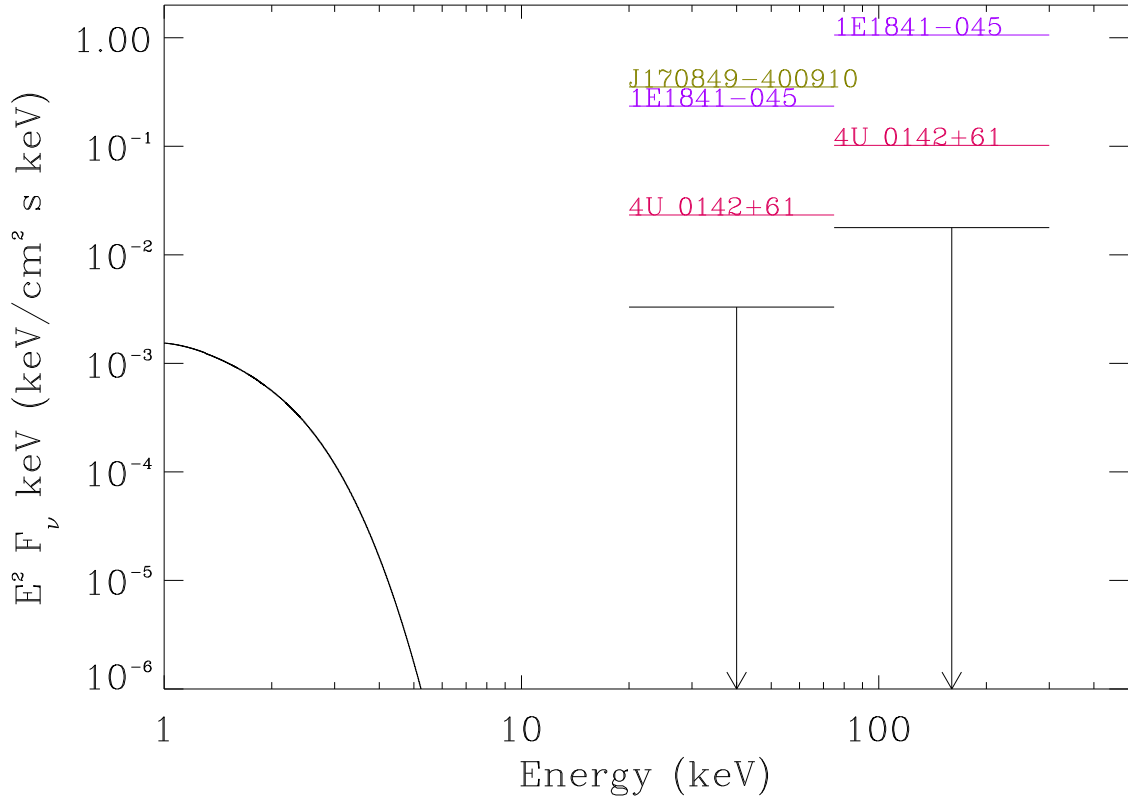


Fig. 1.— The spectrum of the source 1E1207.4–5209. AXPs hard energy fluxes obtained from literature and normalized to a distance of 2 kpc (see Table 4 for references). Solid line indicated soft X-ray spectrum of the CCO which obtained with *XMM-Newton* data, see Table 3 for details. Arrows show the upper limits which we calculated using *INTEGRAL* data.

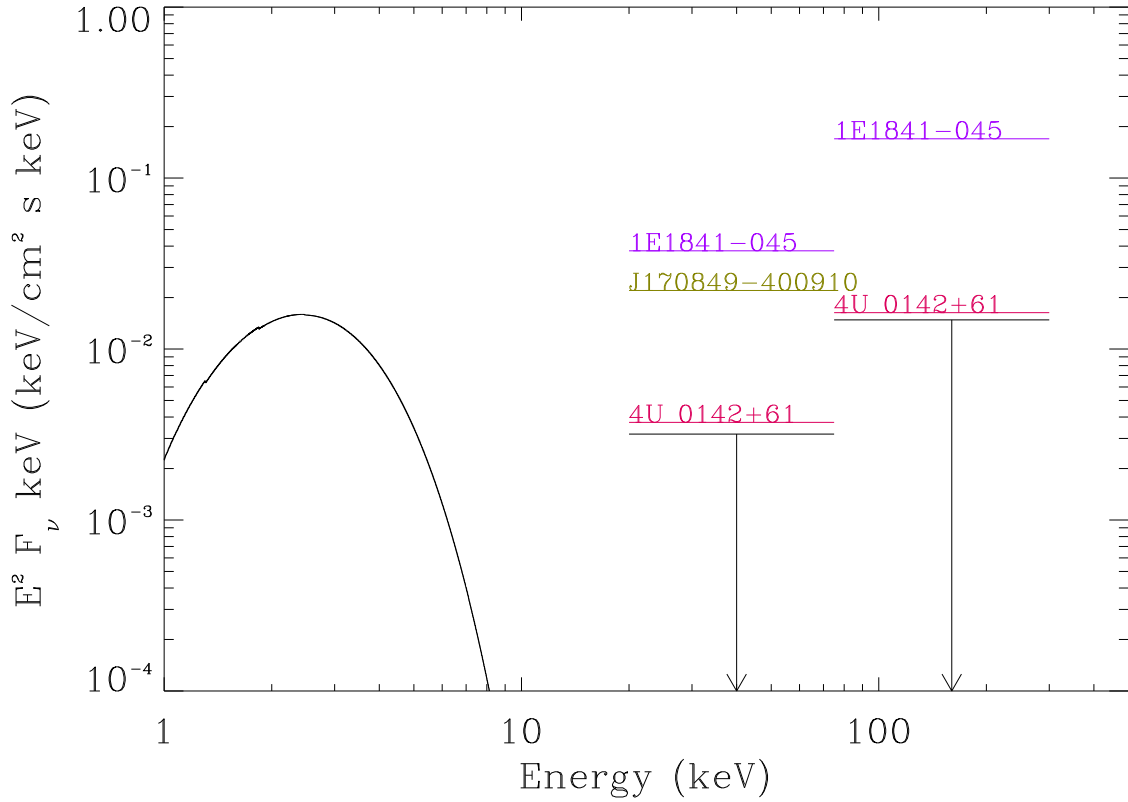


Fig. 2.— The spectrum of the source 1WGA J1713–3949. AXPs hard energy fluxes obtained from literature and normalized to a distance of 5 kpc (see Table 4 for references). Solid line indicated soft X-ray spectrum of the CCO which obtained with *XMM-Newton* data, see Table 3 for details. Arrows show the upper limits which we calculated using *INTEGRAL* data.

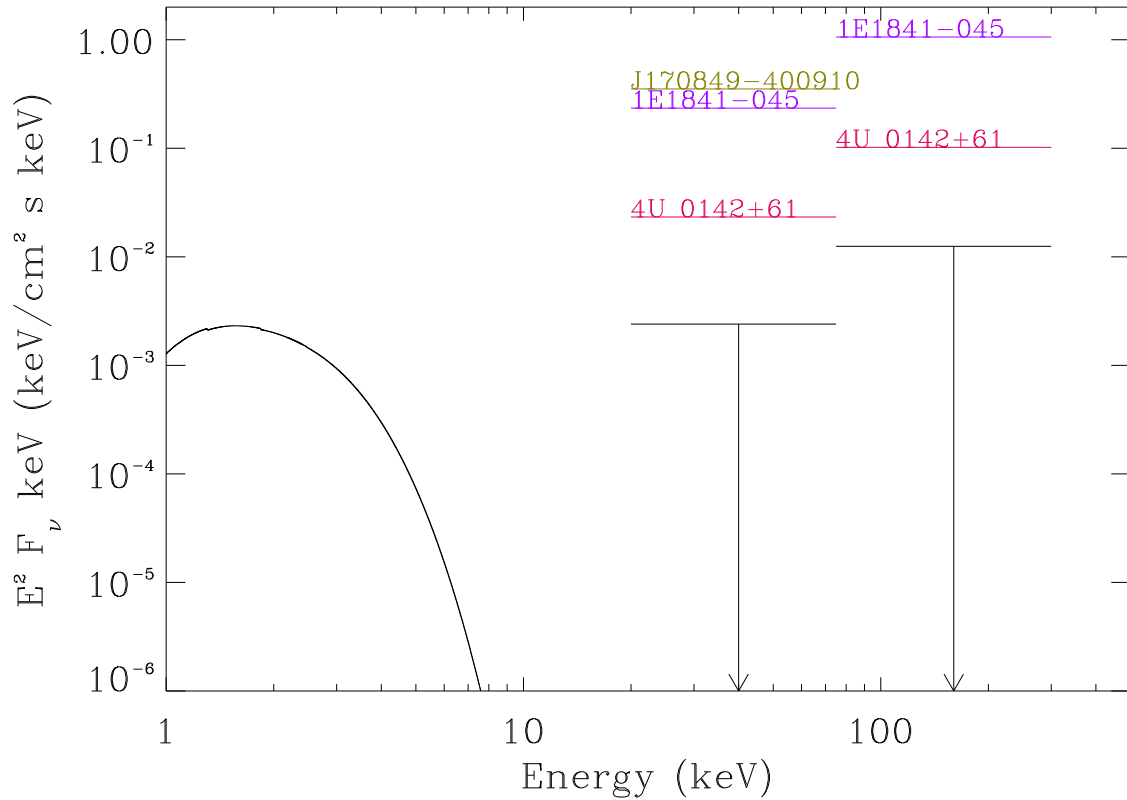


Fig. 3.— The spectrum of the source J082157.5–430017. AXPs hard energy fluxes obtained from literature and normalized to a distance of 2 kpc (see Table 4 for references). Solid line indicated soft X-ray spectrum of the CCO which obtained with *XMM-Newton* data, see Table 3 for details. Arrows show the upper limits which we calculated using *INTEGRAL* data.

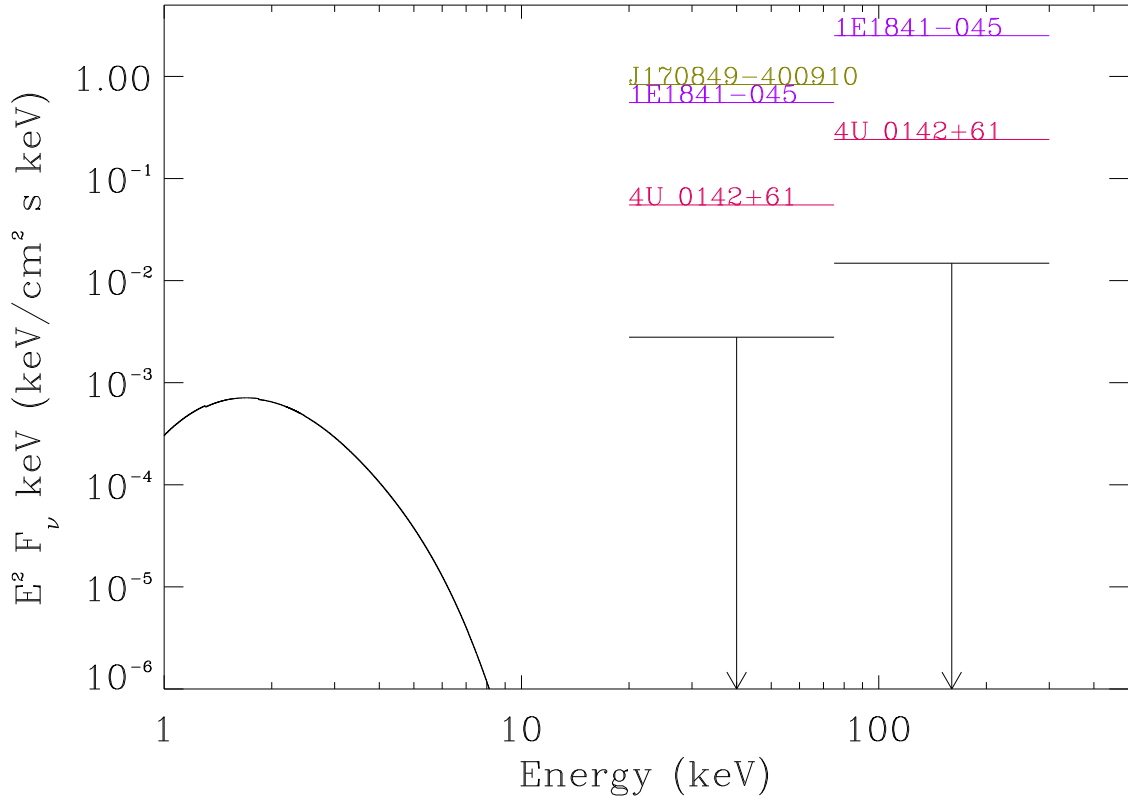


Fig. 4.— The spectrum of the source J085201.4–461753. AXPs hard energy fluxes obtained from literature and normalized to a distance of 1.3 kpc (see Table 4 for references). Solid line indicated soft X-ray spectrum of the CCO which obtained with *XMM-Newton* data, see Table 3 for details. Arrows show the upper limits which we calculated using *INTEGRAL* data.

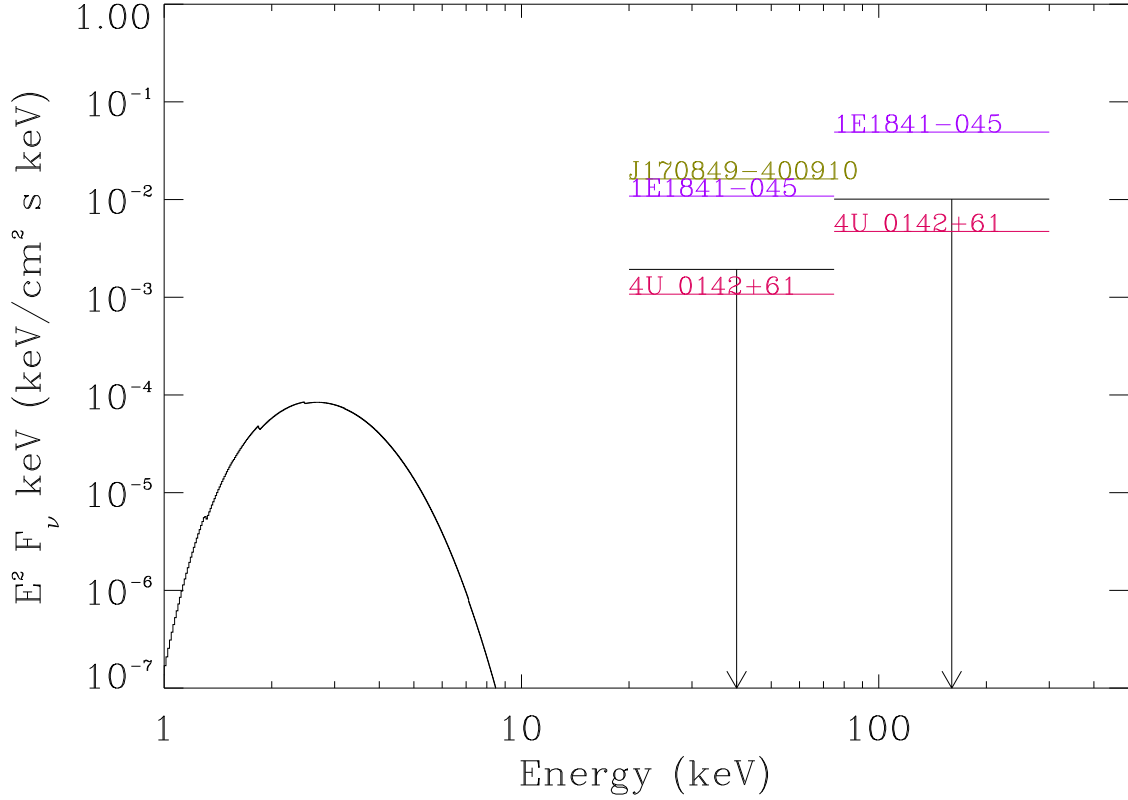


Fig. 5.— The spectrum of the source J1601–5133. AXPs hard energy fluxes obtained from literature and normalized to a distance of 9.3 kpc (see Table 4 for references). Solid line indicated soft X-ray spectrum of the CCO which obtained with *Chandra* data, see Table 3 for details. Arrows show the upper limits which we calculated using *INTEGRAL* data.

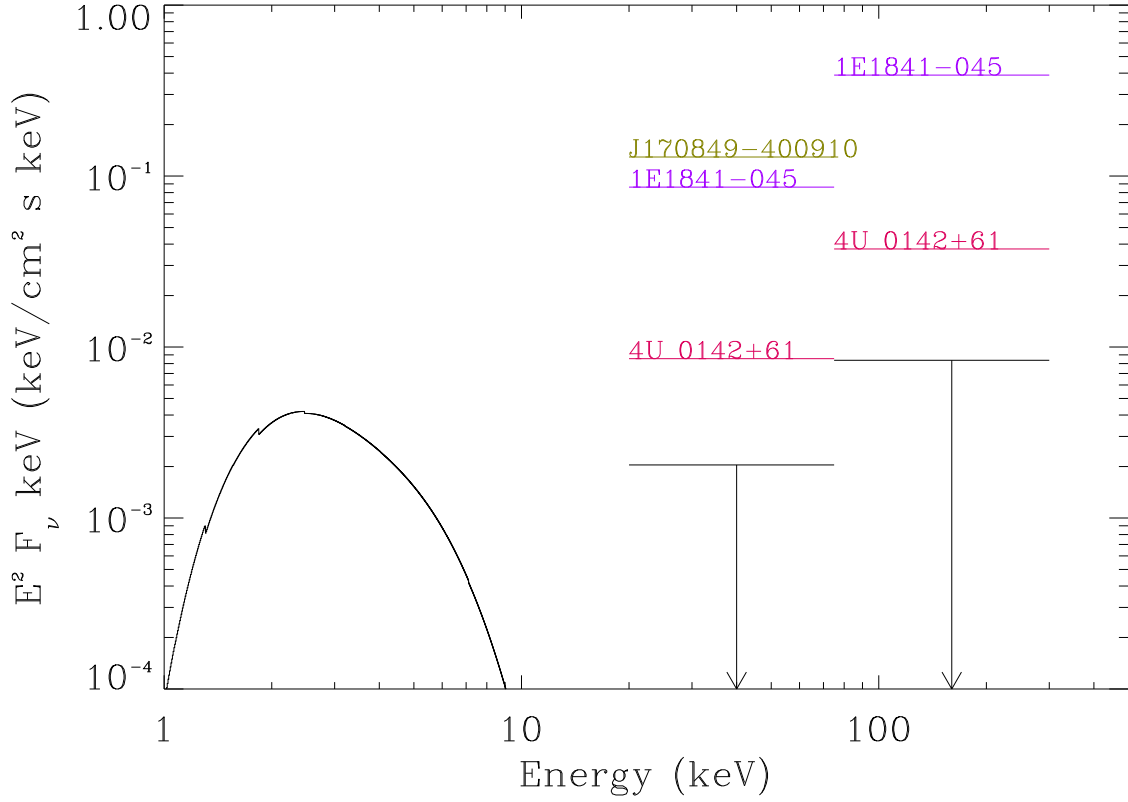


Fig. 6.— The spectrum of the source J161348–5055. AXPs hard energy fluxes obtained from literature and normalized to a distance of 3.3 kpc (see Table 4 for references). Solid line indicated soft X-ray spectrum of the CCO which obtained with *XMM-Newton* data, see Table 3 for details. Arrows show the upper limits which we calculated using *INTEGRAL* data.

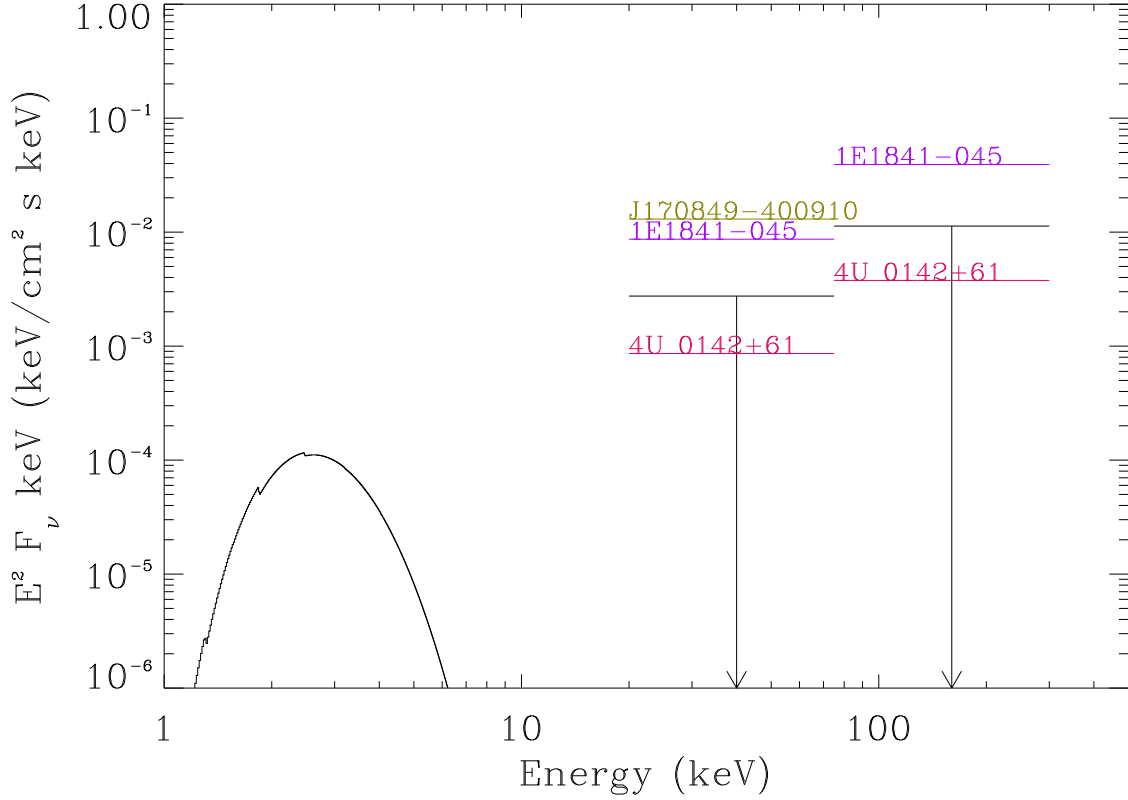


Fig. 7.— The spectrum of the source J181852.0–150213. AXPs hard energy fluxes obtained from literature and normalized to a distance of 10.4 kpc (see Table 4 for references). Solid line indicated soft X-ray spectrum of the CCO which obtained with *Chandra* data, see Table 3 for details. Arrows show the upper limits which we calculated using *INTEGRAL* data.

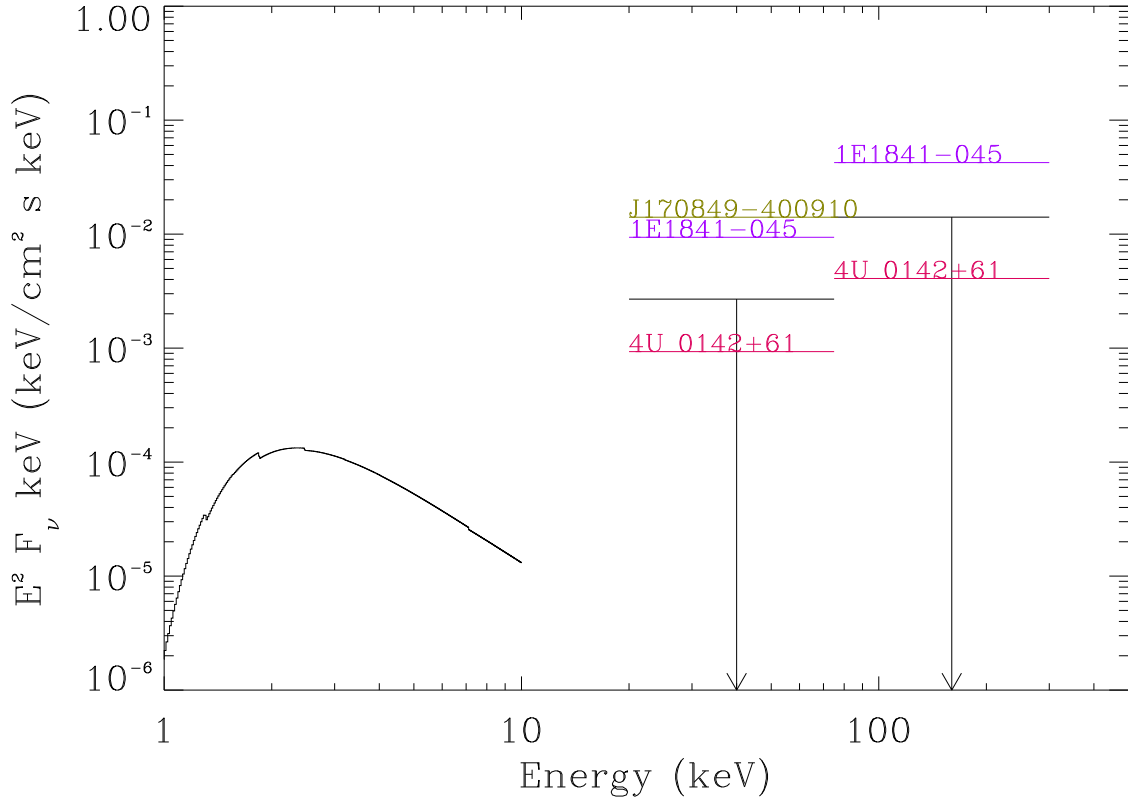


Fig. 8.— The spectrum of the source J185238.6+004020. AXPs hard energy fluxes obtained from literature and normalized to a distance of 7 kpc (see Table 4 for references). Solid line indicated soft X-ray spectrum of the CCO which obtained with *Chandra* data, see Table 3 for details. Arrows show the upper limits which we calculated using *INTEGRAL* data.

Table 1: Integral Observations of CCOs

| Object Name | Begin Date | End Date | Exposure (s) |
|------------------|------------|----------|--------------|
| 1 E1207.4–5209 | 2003-03 | 2005-08 | 1055898 |
| 1WGA J1713–3949 | 2003-02 | 2004-11 | 2152997 |
| J082157.5–430017 | 2003-03 | 2004-12 | 2010543 |
| J085201.4–461753 | 2003-02 | 2004-12 | 1501845 |
| J1601–5133 | 2003-03 | 2005-09 | 4191831 |
| J161348–5055 | 2003-01 | 2005-02 | 4482655 |
| J181852.0–150213 | 1999-12 | 2006-04 | 2807728 |
| J185238.6+004020 | 2003-03 | 2004-11 | 2119644 |
| J232327.9+584843 | 2003-03 | 2004-11 | 1690984 |

Table 2: Properties of CCOs

| Object Name | SNR | Angular size (') | Distance (kpc) | Age (kyr) | Period (s) |
|-------------------------------|--------------------------|------------------|---------------------------------|----------------|------------|
| 1 E1207.4–5209 ^c | G296.5+10.0 | 90 × 65 | 2, 1.5, 1.6-3.3, 2.1, 2 adopted | 3-20 | 0.4 |
| 1WGA J1713–3949 ^c | G347.3–0.5 | 65 × 55 | 5±0.2 | 1-3 | |
| J082157.5–430017 ^b | Puppis A (G260.4–3.4) | 60 × 50 | 2 adopted | 3-4 | |
| J085201.4–461753 ^b | Vela Junior (G266.1–1.2) | 120 | 200 pc, <1, 1.5, 1.3 adopted | 1-3 | |
| J1601–5133 ^c | G330.2+1.0 | 11 | 9.3 | | 7.5 |
| J161348–5055 | RCW 103 (G332.4–0.4) | 10 | 4, 3.3, 4.7, 3.3 adopted | 2 | 6.4 hr |
| J181852.0–150213 ^a | G15.9+0.2 | 7 × 5 | 10.4 | 1 ^d | |
| J185238.6+004020 ^a | Kes 79 (G33.6+0.1) | 10 | ~10, 10±2, 10 adopted | 5-8 | 0.1 |
| J232327.9+584843 ^b | Cas A (G111.7–2.1) | 5 | 3.4 | 0.3 | |

^a Guseinov et al. (2003) ^b Guseinov et al. (2004a) ^c Guseinov et al. (2004b) ^d Reynolds et al. (2006)

Table 3: Model Parameters of CCOs

| Object Name | Model | $N_H(10^{22}cm^{-2})$ | Γ | kT (keV) | $F_x(ergcm^{-2}s^{-1})$ |
|-------------------------------|----------|-----------------------|----------|--|---------------------------------------|
| 1 E1207.4–5209 ^a | BB + BB | 0.1 | | T ₁ = 0.164 T ₂ = 0.319 | 2.24×10^{-12} (0.3 – 4 keV) |
| 1WGA J1713–3949 ^b | BB+BB | 0.47 | | T ₁ = 0.57 T ₂ = 0.32 | - |
| J082157.5–430017 ^c | BB+BB | 0.45 | | T ₁ = 0.225 T ₂ = 0.434 | 8.94×10^{-12} (0.5 – 10 keV) |
| J085201.4–461753 ^d | BB + BB | 3.819 | | T ₁ = 0.34 T ₂ = 0.57 | 2.11×10^{-12} (0.5 – 10 keV) |
| J1601–5133 ^e | BB | 2.5 | | 0.49 | 1.17×10^{-13} (1 – 7 keV) |
| J161348–5055 ^f | BB+BB | 1.5 – 1.8 | | T ₁ = 0.4 T ₂ = 0.8 | - |
| J181852.0–150213 ^g | PL or BB | 4 | 4 | 0.4 | 1×10^{-13} (2 – 9.5 keV) |
| J185238.6+004020 ^h | PL | 2.6 | 4.1 | | 2×10^{-13} (1 – 5 keV) |

^a Luca et al. (2004) ^b Cassam-Chenai et al. (2004) ^c Hui & Becker (2006) ^d Becker et al. (2006) ^e Park et al. (2006) ^f Becker & Aschenbach (2002) ^g Reynolds et al. (2006) ^h Halpern et al. (2007)

Table 4: Hard X-ray luminosity of AXPs

| Object Name | Distance | Flux _{20--75keV} ($erg/cm^2/s$) | Flux _{75--300keV} ($erg/cm^2/s$) | Luminosity _{20--75keV} (erg / s) | Luminosity _{75--300keV} (erg / s) |
|-----------------------------|----------|--|---|---|--|
| 4U 0142+61 ^a | > 2.5 | 2.4×10^{-11} | 1.1×10^{-10} | $> 1.8 \times 10^{34}$ | $> 7.8 \times 10^{34}$ |
| J170849-400910 ^b | 8 | 3.5×10^{-11} | | 2.7×10^{35} | |
| 1E 1841-045 ^c | 6.7 | 3.3×10^{-11} | 1.5×10^{-10} | 1.8×10^{35} | 8.1×10^{34} |

^a den Hartog et al. (2004) ^b Revnivtsev et al. (2004) ^c Molkov et al. (2004)

Table 5: Flux and Luminosity Upper Limits of CCOs

| Object Name | Exposure (s) | Flux _{20–75(KeV)} (MeV/cm ² /s) | Luminosity _{20–75(KeV)} erg / s | Flux _{75–300(KeV)} (MeV/cm ² /s) | Luminosity _{75–300(KeV)} erg / s |
|------------------|--------------|--|---|---|--|
| 1E 1207.4–5209 | 1055898 | 3.3×10^{-6} | 2.5×10^{33} | 1.8×10^{-5} | 1.4×10^{34} |
| 1WGA J1713–3949 | 2152997 | 3.2×10^{-6} | 1.5×10^{34} | 1.5×10^{-5} | 7.1×10^{34} |
| J082157.5–430017 | 2010543 | 2.4×10^{-6} | 1.8×10^{33} | 1.3×10^{-5} | 9.6×10^{33} |
| J085201.4–461753 | 1501845 | 2.8×10^{-6} | 9.0×10^{32} | 1.5×10^{-5} | 4.8×10^{33} |
| J1601–5133 | 4191831 | 1.9×10^{-6} | 3.2×10^{34} | 1.0×10^{-5} | 1.7×10^{35} |
| J161348–5055 | 4482655 | 2.0×10^{-6} | 4.3×10^{33} | 8.4×10^{-6} | 1.7×10^{34} |
| J181852.0–150213 | 2807728 | 2.8×10^{-6} | 5.7×10^{34} | 1.1×10^{-5} | 2.3×10^{35} |
| J185238.6+004020 | 2119644 | 2.7×10^{-6} | 2.5×10^{34} | 1.4×10^{-5} | 1.3×10^{35} |
| J232327.9+584843 | 1690984 | - | - | 1.4×10^{-5} | 3.1×10^{34} |